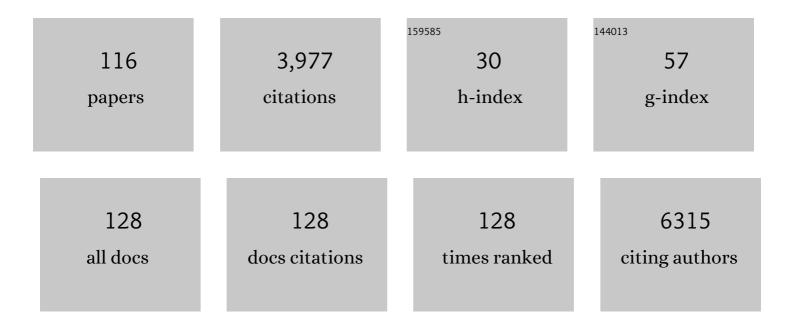
Yingying Wang

List of Publications by Year in descending order

Source: https://exaly.com/author-pdf/718727/publications.pdf Version: 2024-02-01



#	Article	IF	CITATIONS
1	Clearance of senescent cells by ABT263 rejuvenates aged hematopoietic stem cells in mice. Nature Medicine, 2016, 22, 78-83.	30.7	1,273
2	Echinochloa crus-galli genome analysis provides insight into its adaptation and invasiveness as a weed. Nature Communications, 2017, 8, 1031.	12.8	138
3	Development of Tract-Specific White Matter Pathways During Early Reading Development in At-Risk Children and Typical Controls. Cerebral Cortex, 2017, 27, bhw095.	2.9	96
4	Sex differences in white matter development during adolescence: A DTI study. Brain Research, 2012, 1478, 1-15.	2.2	93
5	Room temperature H2S gas sensing properties of In2O3 micro/nanostructured porous thin film and hydrolyzation-induced enhanced sensing mechanism. Sensors and Actuators B: Chemical, 2016, 228, 74-84.	7.8	90
6	Biodegradation of benzo(a)pyrene by Microbacterium sp. strain under denitrification: Degradation pathway and effects of limiting electron acceptors or carbon source. Biochemical Engineering Journal, 2017, 121, 131-138.	3.6	84
7	Frequency andÂspatial characteristics ofÂhigh-frequency neuromagnetic signals inÂchildhood epilepsy. Epileptic Disorders, 2009, 11, 113-125.	1.3	75
8	Hyaluronic-Acid-Based pH-Sensitive Nanogels for Tumor-Targeted Drug Delivery. ACS Biomaterials Science and Engineering, 2017, 3, 2410-2419.	5.2	61
9	Noninvasive localization of epileptogenic zones with ictal high-frequency neuromagnetic signals. Journal of Neurosurgery: Pediatrics, 2010, 5, 113-122.	1.3	59
10	Increased resting-state functional connectivity of visual- and cognitive-control brain networks after training in children with reading difficulties. NeuroImage: Clinical, 2015, 8, 619-630.	2.7	56
11	The relationship between socioeconomic status and white matter microstructure in preâ€reading children: A longitudinal investigation. Human Brain Mapping, 2019, 40, 741-754.	3.6	54
12	Amorphous NiP as cocatalyst for photocatalytic water splitting. Ceramics International, 2018, 44, 5459-5465.	4.8	53
13	Photothermal CO detection in a hollow-core negative curvature fiber. Optics Letters, 2019, 44, 4048.	3.3	52
14	Examining the relationship between home literacy environment and neural correlates of phonological processing in beginning readers with and without a familial risk for dyslexia: an fMRI study. Annals of Dyslexia, 2016, 66, 337-360.	1.7	51
15	Involvement of the right hemisphere in reading comprehension: A DTI study. Brain Research, 2014, 1582, 34-44.	2.2	49
16	Effects of ceramic particle size on microstructure and the corrosion behavior of cold sprayed SiCp/Al 5056 composite coatings. Surface and Coatings Technology, 2017, 315, 314-325.	4.8	48
17	Reading acceleration training changes brain circuitry in children with reading difficulties. Brain and Behavior, 2014, 4, 886-902.	2.2	47
18	lmmunogenicity of a cell culture-derived inactivated vaccine against a common virulent isolate of grass carp reovirus. Fish and Shellfish Immunology, 2016, 54, 473-480.	3.6	46

#	Article	IF	CITATIONS
19	Dataâ€Driven Identification of Hydrogen Sulfide Scavengers. Angewandte Chemie - International Edition, 2019, 58, 10898-10902.	13.8	43
20	Lessons to be learned: how a comprehensive neurobiological framework of atypical reading development can inform educational practice. Current Opinion in Behavioral Sciences, 2016, 10, 45-58.	3.9	42
21	Curative or pre-emptive adenovirus-specific T cell transfer from matched unrelated or third party haploidentical donors after HSCT, including UCB transplantations: a successful phase I/II multicenter clinical trial. Journal of Hematology and Oncology, 2017, 10, 102.	17.0	39
22	Oral delivery of Bacillus subtilis spores expressing grass carp reovirus VP4 protein produces protection against grass carp reovirus infection. Fish and Shellfish Immunology, 2019, 84, 768-780.	3.6	39
23	Wideband <inline-formula> <tex-math notation="LaTeX">\$N\$</tex-math> </inline-formula> -Beam Arrays Using Low-Complexity Algorithms and Mixed-Signal Integrated Circuits. IEEE Journal on Selected Topics in Signal Processing, 2018, 12, 368-382.	10.8	38
24	High Gamma Oscillations of Sensorimotor Cortex During Unilateral Movement in the Developing Brain: a MEG Study. Brain Topography, 2011, 23, 375-384.	1.8	37
25	Strategies for the Design of Donors and Precursors of Reactive Sulfur Species. Chemistry - A European Journal, 2019, 25, 4005-4016.	3.3	37
26	Modeling the Developmental Patterns of Auditory Evoked Magnetic Fields in Children. PLoS ONE, 2009, 4, e4811.	2.5	37
27	Effect of desertification on productivity in a desert steppe. Scientific Reports, 2016, 6, 27839.	3.3	35
28	Effect of atomic mobility on the electrochemical properties of a Zr58Nb3Cu16Ni13Al10 bulk metallic glass. Electrochimica Acta, 2018, 267, 222-233.	5.2	35
29	Biomimetic cartilage scaffold with orientated porous structure of two factors for cartilage repair of knee osteoarthritis. Artificial Cells, Nanomedicine and Biotechnology, 2019, 47, 1710-1721.	2.8	34
30	Interictal magnetoencephalographic findings related with surgical outcomes in lesional and nonlesional neocortical epilepsy. Seizure: the Journal of the British Epilepsy Association, 2011, 20, 692-700.	2.0	32
31	Gamma oscillations in the primary motor cortex studied with MEG. Brain and Development, 2010, 32, 619-624.	1.1	31
32	DNA Polymerase-Directed Hairpin Assembly for Targeted Drug Delivery and Amplified Biosensing. ACS Applied Materials & Interfaces, 2016, 8, 26532-26540.	8.0	31
33	White matter differences between multiple system atrophy (parkinsonian type) and Parkinson's disease: A diffusion tensor image study. Neuroscience, 2015, 305, 109-116.	2.3	30
34	Ultrasmall Ru Nanoclusters on Nitrogenâ€Enriched Hierarchically Porous Carbon Support as Remarkably Active Catalysts for Hydrolysis of Ammonia Borane. ChemCatChem, 2018, 10, 4910-4916.	3.7	30
35	The relationship between biological and psychosocial risk factors and restingâ€state functional connectivity in 2â€monthâ€old Bangladeshi infants: A feasibility and pilot study. Developmental Science, 2019, 22, e12841.	2.4	30
36	Time, frequency and volumetric differences of high-frequency neuromagnetic oscillation between left and right somatosensory cortices. International Journal of Psychophysiology, 2009, 72, 102-110.	1.0	28

#	Article	IF	CITATIONS
37	Effects of learning experience on forgetting rates of item and associative memories. Learning and Memory, 2016, 23, 365-378.	1.3	28
38	Multifactorial pathways facilitate resilience among kindergarteners at risk for dyslexia: A longitudinal behavioral and neuroimaging study. Developmental Science, 2021, 24, e12983.	2.4	28
39	Neuromagnetic correlates of developmental changes in endogenous high-frequency brain oscillations in children: A wavelet-based beamformer study. Brain Research, 2009, 1274, 28-39.	2.2	27
40	Cue-independent forgetting by intentional suppression – Evidence for inhibition as the mechanism of intentional forgetting. Cognition, 2015, 143, 31-35.	2.2	25
41	In situ synthesis of porous array films on a filament induced micro-gap electrode pair and their use as resistance-type gas sensors with enhanced performances. Nanoscale, 2015, 7, 14264-14271.	5.6	24
42	Neuromagnetic measures of word processing in bilinguals and monolinguals. Clinical Neurophysiology, 2011, 122, 1706-1717.	1.5	23
43	Phosphatidylinositol 3â€kinase β and β isoforms play key roles in metastasis of prostate cancer DU145 cells. FASEB Journal, 2018, 32, 5967-5975.	0.5	23
44	Graphene Oxide and Lysozyme Ultrathin Films with Strong Antibacterial and Enhanced Osteogenesis. Langmuir, 2019, 35, 6752-6761.	3.5	23
45	The performance of a community-based colorectal cancer screening program: Evidence from Shanghai Pudong New Area, China. Preventive Medicine, 2019, 118, 243-250.	3.4	23
46	Experimental and Theoretical Study on the Synergistic Inhibition Effect of Pyridine Derivatives and Sulfur-Containing Compounds on the Corrosion of Carbon Steel in CO2-Saturated 3.5 wt.% NaCl Solution. Molecules, 2018, 23, 3270.	3.8	22
47	Predicting domain-specific actions in expert table tennis players activates the semantic brain network. NeuroImage, 2019, 200, 482-489.	4.2	21
48	Neuromagnetic evidence of impaired cortical auditory processing in pediatric intractable epilepsy. Epilepsy Research, 2010, 92, 63-73.	1.6	20
49	Impaired Auditory Information Processing During Acute Migraine: A Magnetoencephalography Study. International Journal of Neuroscience, 2011, 121, 355-365.	1.6	20
50	Comparative Study on Physical–Chemical and Biological Characteristics of Grass Carp Reovirus From Different Genotypes. Journal of the World Aquaculture Society, 2016, 47, 862-872.	2.4	20
51	Development of indirect immunofluorescence assay for TCID50 measurement of grass carp reovirus genotype II without cytopathic effect onto cells. Microbial Pathogenesis, 2018, 114, 68-74.	2.9	20
52	Aberrant high-gamma oscillations in the somatosensory cortex of children with cerebral palsy: A meg study. Brain and Development, 2012, 34, 576-583.	1.1	19
53	Investigating the Influences of Language Delay and/or Familial Risk for Dyslexia on Brain Structure in 5-Year-Olds. Cerebral Cortex, 2015, 27, bhv267.	2.9	19
54	Central But Not General Obesity Is Positively Associated with the Risk of Hyperhomocysteinemia in Middle-Aged Women. Nutrients, 2019, 11, 1614.	4.1	19

#	Article	IF	CITATIONS
55	Comparison of Activity, Expression, and S-Nitrosylation of Calcium Transfer Proteins between Pale, Soft, and Exudative and Red, Firm, and Non-exudative Pork during Post-Mortem Aging. Journal of Agricultural and Food Chemistry, 2019, 67, 3242-3248.	5.2	19
56	ldentification of Abnormal Neuromagnetic Signatures in the Motor Cortex of Adolescent Migraine. Headache, 2010, 50, 1005-1016.	3.9	18
57	Concordance of MEG and fMRI patterns in adolescents during verb generation. Brain Research, 2012, 1447, 79-90.	2.2	18
58	Comparative proteomic analysis and characterization of benzo(a)pyrene removal by Microbacterium sp. strain M.CSW3 under denitrifying conditions. Bioprocess and Biosystems Engineering, 2017, 40, 1825-1838.	3.4	18
59	Gas-Sensing Mechanism of Silica with Photonic Bandgap Shift. Analytical Chemistry, 2019, 91, 1133-1139.	6.5	18
60	Neural substrates of the executive function construct, ageâ€related changes, and task materials in adolescents and adults: ALE metaâ€analyses of 408 fMRI studies. Developmental Science, 2021, 24, e13111.	2.4	18
61	Porosity Characterization of Cold Sprayed Stainless Steel Coating Using Three-Dimensional X-ray Microtomography. Coatings, 2018, 8, 326.	2.6	17
62	Spatiotemporal and frequency signatures of word recognition in the developing brain: A magnetoencephalographic study. Brain Research, 2013, 1498, 20-32.	2.2	16
63	Co-delivery of hydrophilic gemcitabine and hydrophobic paclitaxel into novel polymeric micelles for cancer treatment. RSC Advances, 2017, 7, 24030-24039.	3.6	15
64	The interaction between state and dispositional emotions in decision making: An ERP study. Biological Psychology, 2017, 123, 126-135.	2.2	15
65	Acid-labile poly(ethylene glycol) shell of hydrazone-containing biodegradable polymeric micelles facilitating anticancer drug delivery. Journal of Bioactive and Compatible Polymers, 2018, 33, 119-133.	2.1	15
66	Comparison of long-term outcomes of young patients after a coronary event associated with familial hypercholesterolemia. Lipids in Health and Disease, 2019, 18, 131.	3.0	15
67	Magnetoencephalography reveals altered auditory information processing in youth with obsessive-compulsive disorder. Psychiatry Research - Neuroimaging, 2013, 212, 132-140.	1.8	14
68	Molecular detection of genotype II grass carp reovirus based on nucleic acid sequence-based amplification combined with enzyme-linked immunosorbent assay (NASBA-ELISA). Journal of Virological Methods, 2017, 243, 92-97.	2.1	14
69	Corrosion resistance mechanism of palladium film-plated stainless steel in boiling H 2 SO 4 solution. Corrosion Science, 2018, 135, 222-232.	6.6	14
70	Synthesis of Unsymmetric Trisulfides from 9-Fluorenylmethyl Disulfides. Organic Letters, 2018, 20, 465-468.	4.6	14
71	Acyl Selenyl Sulfides as the Precursors for Reactive Sulfur Species (Hydrogen Sulfide, Polysulfide,) Tj ETQq1 1 0.7	'84314 rgl 4.6	3T /Overlock
72	Meta-Analytic Findings on Reading in Children With Cochlear Implants. Journal of Deaf Studies and	1.2	13

Deaf Education, 2021, 26, 336-350.

1.213

#	Article	IF	CITATIONS
73	Aberrant Neuromagnetic Activation in the Motor Cortex in Children with Acute Migraine: A Magnetoencephalography Study. PLoS ONE, 2012, 7, e50095.	2.5	13
74	Spatial and Frequency Differences of Neuromagnetic Activities Between the Perception of Open- and Closed-class Words. Brain Topography, 2008, 21, 75-85.	1.8	12
75	Neuromagnetic biomarkers of visuocortical development in healthy children. Clinical Neurophysiology, 2010, 121, 1555-1562.	1.5	12
76	Comparison of Functional Network Connectivity for Passive-Listening and Active-Response Narrative Comprehension in Adolescents. Brain Connectivity, 2014, 4, 273-285.	1.7	12
77	Neural Bases of Phonological and Semantic Processing in Early Childhood. Brain Connectivity, 2020, 10, 212-223.	1.7	12
78	Neural encoding of saltatory pneumotactile velocity in human glabrous hand. PLoS ONE, 2017, 12, e0183532.	2.5	12
79	Spatial and Frequency Differences of Neuromagnetic Activities in Processing Concrete and Abstract Words. Brain Topography, 2008, 20, 123-129.	1.8	11
80	SRT contributes significantly to sludge reduction in the OSA-based activated sludge process. Environmental Technology (United Kingdom), 2017, 38, 305-315.	2.2	11
81	Brain encoding of saltatory velocity through a pulsed pneumotactile array in the lower face. Brain Research, 2017, 1677, 58-73.	2.2	11
82	Gene Modules Co-regulated with Biosynthetic Gene Clusters for Allelopathy between Rice and Barnyardgrass. International Journal of Molecular Sciences, 2019, 20, 3846.	4.1	9
83	Long noncoding RNA CCDC144NL-AS1 knockdown induces naÃ ⁻ ve-like state conversion of human pluripotent stem cells. Stem Cell Research and Therapy, 2019, 10, 220.	5.5	9
84	Multioctave supercontinua from shock-coupled soliton self-compression. Physical Review A, 2019, 99, .	2.5	9
85	28 Si total body irradiation injures bone marrow hematopoietic stem cells via induction of cellular apoptosis. Life Sciences in Space Research, 2017, 13, 39-44.	2.3	8
86	An intelligent wearable device for human's cervical vertebra posture monitoring. , 2018, 2018, 3280-3283.		8
87	Brain lateralization in children with upper-limb reduction deficiency. Journal of NeuroEngineering and Rehabilitation, 2021, 18, 24.	4.6	8
88	Investigation of latent infections caused by cyprinid herpesvirus 3 in koi (<i>Cyprinus carpio</i>) in southern China. Journal of Veterinary Diagnostic Investigation, 2017, 29, 366-369.	1.1	7
89	Metabolomics profiling in a mouse model reveals protective effect of Sancao granule on Con A-Induced liver injury. Journal of Ethnopharmacology, 2019, 238, 111838.	4.1	7
90	Adenovirus-specific T-cell Subsets in Human Peripheral Blood and After IFN-Î ³ Immunomagnetic Selection. Journal of Immunotherapy, 2016, 39, 27-35.	2.4	6

#	Article	IF	CITATIONS
91	Brillouin-based dual-frequency microwave signals generation using polarization-multiplexing modulation. Optics Express, 2019, 27, 24847.	3.4	6
92	Temporal plus epilepsies: Electrophysiology studied with interictal magnetoencephalography and intracranial video-EEG monitoring. Seizure: the Journal of the British Epilepsy Association, 2013, 22, 164-167.	2.0	5
93	Combined ion exchange and adsorption equilibria of 5′-ribonucleotides on the strong acid cation exchange resin NH-1. Journal of Chemical Technology and Biotechnology, 2017, 92, 1678-1689.	3.2	5
94	Functional Connectivity Evoked by Orofacial Tactile Perception of Velocity. Frontiers in Neuroscience, 2020, 14, 182.	2.8	5
95	Frequency-spatial beamformer for MEG source localization. Biomedical Signal Processing and Control, 2015, 18, 263-273.	5.7	4
96	One-step synthesis of magnetic-TiO2-nanocomposites with high iron oxide-composing ratio for photocatalysis of rhodamine 6G. PLoS ONE, 2019, 14, e0221221.	2.5	4
97	Walk the talk: coordinating gesture with locomotion for conversational characters. Computer Animation and Virtual Worlds, 2016, 27, 369-377.	1.2	3
98	Automated design and optimization of integrated inductors and transformers. , 2016, , .		3
99	Volumetric localization of epileptic activity using wavelet-based synthetic aperture magnetometry. International Congress Series, 2007, 1300, 697-700.	0.2	2
100	Detection of koi herpesvirus (KHV) using a monoclonal antibody against Cyprinus carpio IgM. Archives of Virology, 2017, 162, 2381-2385.	2.1	2
101	Indoor Occupancy Awareness and Localization Using Passive Electric Field Sensing. , 2018, , .		2
102	Changes in Sensorimotor Cortical Activation in Children Using Prostheses and Prosthetic Simulators. Brain Sciences, 2021, 11, 991.	2.3	2
103	Bayesian MEG time courses with fMRI priors. Brain Imaging and Behavior, 2022, 16, 781-791.	2.1	2
104	Detection of subtle structural abnormality in tuberous sclerosis using MEG guided post-image processing. International Congress Series, 2007, 1300, 693-696.	0.2	1
105	MEG source localization using a frequency beamformer. , 2010, , .		1
106	Physical Feature Encoding and Word Recognition Abilities Are Altered in Children with Intractable Epilepsy: Preliminary Neuromagnetic Evidence. Behavioural Neurology, 2015, 2015, 1-10.	2.1	1
107	Efficient Dispersive Waves Generation From Argon-Filled Anti-Resonant Nodeless Fiber. , 2017, , .		1
108	Emergent Reading and Brain Development. , 0, , .		1

#	Article	IF	CITATIONS
109	A switched-capacitor-based low-power receiver for electrocardiogram and respiration rate detection. Analog Integrated Circuits and Signal Processing, 2019, 99, 437-446.	1.4	1
110	Deep Sequencing-Based Transcriptome Analysis Reveals the Regulatory Mechanism of Bemisia tabaci (Hemiptera: Aleyrodidae) Nymph Parasitized by Encarsia sophia (Hymenoptera: Aphelinidae). PLoS ONE, 2016, 11, e0157684.	2.5	1
111	Spatially distributed sequential array stimulation of tibial anterior muscle for foot drop correction. , 2015, 2015, 3407-10.		0
112	\$\$varvec{varDelta }\$\$–\$\$varvec{varSigma }\$\$ noise-shaping in 3-D space–time for 2-D wideband antenna array receivers. Multidimensional Systems and Signal Processing, 2019, 30, 1609-1631.	2.6	0
113	Effect of aeration rates on the performance of an OSA-based sludge reduction process: limitations and implications. , 0, 76, 166-173.		0
114	Identification and development of a polyclonal antibody against proteins encoded by the <i>ORF136</i> gene in Cyprinid herpesvirus 3. Journal of Fishery Sciences of China, 2018, 25, 204.	0.2	0
115	Dynamic causal modeling of sensorimotor networks elicited by saltatory pneumotactile velocity in the glabrous hand. Journal of Neuroimaging, 2022, 32, 752-764.	2.0	0
116	Dynamic causal modeling of neural responses to an orofacial pneumotactile velocity array. NeuroImage Reports, 2022, 2, 100081.	1.0	0